Universal closed-tube barcoding for monitoring the shark and ray trade in megadiverse conservation hotspots

Andhika P. Prasetyo[1,2,3*], Marine Cusa[1,4], Joanna M. Murray[5], Firdaus Agung[6], Efin Muttaqin[7], Stefano Mariani[8†] and Allan D. McDevitt[1,9†*]

1 - School of Science, Engineering and Environment, University of Salford, Salford, UK
2 - Centre Fisheries Research, Ministry for Marine Affairs and Fisheries, Indonesia
3 - Research Centre for Conservation of Marine and Inland Water Resources, National Research and Innovation Agency, Bogor, Indonesia
4 - Oceana Europe, Madrid, Spain
5 - Centre for Environment, Fisheries and Aquaculture Science (CEFAS), Lowestoft, UK
6 - Directorate for Conservation and Marine Biodiversity, Ministry for Marine Affairs and Fisheries, Indonesia
7 - Wildlife Conservation Society Indonesia Program, Indonesia
8 - School of Biological and Environmental Sciences, Liverpool John Moores University, Liverpool, UK
9 - Department of Natural Sciences and the Environment, School of Science and Computing, Atlantic Technological University, Galway, Ireland

* Corresponding author. A. P. Prasetyo (a.p.prasetyo@edu.salford.ac.uk) or A. McDevitt (allan.mcdevitt@atu.ie)

† These authors have joint-last authorship

Highlights

1. We applied a portable, universal, closed-tube DNA barcoding approach originally developed for bony fishes to distinguish between shark and ray species traded in Indonesia.
2. We built a deep machine learning model to automatically assign species from the qPCR fluorescence spectra produced by two barcodes
3. The model achieved 79.41% accuracy for classifying 28 elasmobranch species, despite the barcode regions being designed for teleost species
4. This tool can serve as a potent single-assay *in-situ* diagnostic tool to regulate trade operations and it will be significantly enhanced by further optimisation of the barcode regions to fit elasmobranch DNA sequence variation

Summary

Trade restrictions for many endangered elasmobranch species exist to disincentivise their exploitation and curb their declines. However, the variety of products and the complexity of import/export routes make trade monitoring challenging. We investigate the use of a portable, universal, DNA-based tool which would greatly facilitate *in-situ* monitoring. We collected shark and ray samples across the Island of Java, Indonesia, and selected 28 species (including 22 CITES-listed species) commonly encountered in landing sites and export hubs to test a recently developed real-time PCR single-assay originally developed for screening bony fish. We employed a deep learning algorithm to recognize species based on DNA melt-curve signatures. By combining visual and machine learning assignment methods, we distinguished 25 out of 28 species, 20 of which were CITES-listed. With further refinement, this method can provide a practical tool for monitoring elasmobranch trade worldwide, without the need for a lab or the bespoke design of species-specific assays.

Keywords: elasmobranchs, DNA barcoding, deep learning, illegal trade, biodiversity monitoring, Indonesia.

Introduction

Biodiversity is depleting more rapidly than at any time in human history. Within the last 50 years, animal species have declined by an average of almost 70% due to continued and increasing anthropogenic stressors (Bar-On et al., 2018; Leung et al., 2020). Shark and ray populations (hereafter referred to as ‘elasmobranchs’) have one of the highest extinction risks across the animal kingdom due to fishing pressure, whether targeted or as by-catch (Dulvy et al., 2014; MacNeil et al., 2020; Pacoureau et al., 2021). Although some elasmobranch fisheries can be sustainably managed (Simpfendorfer and Dulvy, 2017), the market demand for shark and ray products typically leads to overexploitation (Clarke et al., 2006; Dulvy et al., 2014).

The rapid global decline of elasmobranch populations requires collaborative management and conservation measures to ensure the long-term benefits of these

populations to the wider ecosystem, including, where sustainable, for human resource use. Binding international trade consortia, such as CITES (Convention on International Trade in Endangered Species of Wild Fauna and Flora), regulate and provide the framework to restrict the international trade of species of priority conservation concern by creating species listing (CITES appendix I and II). Indeed, there has been an increasing number of elasmobranch listings in CITES Appendix II over the last decade with 38 of the 47 species regulated by CITES added at the 16th (2013), 17th (2016) and 18th (2019) Conference of the Parties conventions (Booth et al., 2020). The number of Appendix II listings then more than tripled at the 19th Conference of the Parties (CoP19) in 2022 where parties agreed to add all remaining (54) species of requiem sharks (Carcharhinidae spp.), 6 species of hammerhead sharks, and 37 species of guitarfishes to Appendix II. Seven species of Brazilian freshwater stingrays were also adopted for Appendix II listing. The scale and pace of these listings (now 151 species) present an important implementation challenge for countries with large and diverse landings of sharks and rays, such as Indonesia.

As a result of substantial bycatch, Indonesian fisheries hold the world's largest volume of elasmobranch landings (Fahmi and Dharmadi, 2015; FAO, 2022). This exploitation contributes to the high vulnerability rate of elasmobranch populations in Indonesian waters (Mardhiah et al., 2019), including the populations in its coral reef ecosystems (MacNeil et al., 2020). This is particularly concerning as Indonesia harbours almost a quarter of the world's elasmobranch diversity (Ali et al., 2018; Ali et al., 2014). Despite this, export volumes of elasmobranch products from Indonesia represent only a small fraction of its landing volume (FAO, 2021), which likely reflects its communities' high dependency on shark and ray as an alternative protein source (Dharmadi et al., 2019b; Muttaqin et al., 2018; Prasetyo et al., 2021). Several measures have been established by the Indonesian authorities to reduce the decline of elasmobranch populations, such as: increasing the number of protected species, extensive outreach programmes, improvement of data collection and stock assessment, expansion of marine protected areas, as well as the establishment of port state measures to combat illegal fishing (Booth et al., 2018; Dharmadi et al., 2015; Nugraha et al., 2020; Oktaviyani et al., 2019).

The issue around elasmobranch fisheries is rendered even more challenging by the myriad of shark and ray product derivations, which add another layer of complexity

(Dent and Clarke, 2015; Safari and Hassan, 2020; Shea and To, 2017). Due to their similarity in appearance and the lack of distinctive features in most derivative products, elasmobranch species can be deliberately or accidentally mislabelled by those involved in the trade (**Figure 1**). The general lack of transparency in the trade of living resources is an ongoing concern for fisheries and conservation management (Naaum and Hanner, 2016) and can have a negative impact on stock management, and damages the reputation of entire sectors and countries (Cawthorn and Mariani, 2017; Naaum and Hanner, 2016). Furthermore, the continuous increase of elasmobranch species listed in the CITES Appendices requires constant improvements of national and transnational capabilities in monitoring the supply chain (Pavitt et al., 2021).

The rapid development of DNA-based diagnostic tools offers an ever-expanding option for wildlife identification, which have greatly assisted elasmobranch biology and forensics. Established DNA barcoding (Shivji et al., 2002) and mini-barcoding (Fields et al., 2015) approaches can robustly identify species in fresh and processed samples. However, these traditional DNA barcoding methods require longer processing time and high costs for their sequencing processes. More recently, advances in real-time PCR have eliminated the sequencing stage, thereby allowing species identification to be conducted in the field. This approach uses target-specific primers and fluorescent dyes to detect the presence of the targeted nucleic acid template during PCR amplification and has been successfully applied to detect several CITES-listed shark species in a single run tube (Cardeñosa et al., 2018) and Multiplex LAMP (Lin et al., 2021). However, given their reliance on species-specific primers and probes, these methods are better suited to screening large numbers of specimens from one or few species rather than from a wide variety of species. Thus, the need remains for a fast and easy way to identify any sample, by-passing the need to design species-specific assays.

This issue is particularly glaring when inspectors are dealing with multiple types of products from different species across many locations and with a limited timeframe to investigate species compositions (Prasetyo et al., 2021). This year, the magnitude of the challenge has more than tripled, with the number of CITES-listed species going from 47 to 151 (CITES, 2022; Collyns, 2022). Since CITES regulations still allows species listed on Appendix II to be traded by considering the sustainability of

exploitation through a Non-detrimental Findings (NDF) framework, trade monitoring is more crucial than ever before.

In an attempt to circumvent the limits of species-specific methods, a universal single-tube assay marketed as FASTFISH-ID™ was recently developed for use in the seafood industry (Naaum et al., 2021). This method uses LATE (Linear-After-The-Exponent) PCR to amplify one strand of the full 650bp COI barcoding region (Sanchez et al, 2004), and uses a set of fluorescent probes to target two distinct mini-barcode regions selected for their high intra-specific variability which will then produce unique species-specific fluorescent signatures (Naaum et al., 2021). The fluorescent signatures are then compared to those kept in a cloud-based library of verified specimen signatures.

However, this approach and its libraries were originally designed and validated for bony fishes (Naaum et al., 2021) and no elasmobranch fluorescence fingerprints are publicly available in the FASTFISH-ID™ cloud. We therefore chose to test i) whether the existing FASTFISH-ID™ diagnostics could produce a diverse range of fluorescent signatures unique and specific to each of the 28 elasmobranch species frequently found in Indonesian trade; and ii) whether a deep machine learning method could quantitatively assign signatures to the correct species, irrespective of the visual appearance of the fluorescence. Deep learning algorithms are highly flexible and well suited for undertaking these tasks (LeCun et al., 2015; Malde et al., 2019), and have recently been applied in marine science, including fish size estimation (Garcia et al., 2019), bycatch detection and shark identification from photos and videos (Jenrette et al., 2022; Peña et al., 2021; Sharma et al., 2018). Our findings indicate that this portable, universal methodology performs well even for ‘non-target’ elasmobranch species, and with further refinement, it can become a powerful tool to combat the illegal trade of endangered sharks and rays.

Results

Fluorescent signature of species

After filtering and removing 33 inconsistent runs, 357 pairs of fluorescent signatures from 28 species were generated, including 14 sharks and 14 rays, with 22 of those species (12 sharks, 10 rays) being CITES-listed species. Within 2.5 hours, all types of samples - from fresh to processed samples sourced from different body parts - were amplified and produced one or two fluorescent signatures (referred to as BS1 and BS2 for barcode segment one and barcode segment two) (**Tables S.1 and S.2**. These two barcode segments refer to the two mini-barcode regions within the amplified COI target sequence that emitted fluorescent to be read by the real-time PCR machine.

Many species were distinguishable using a combination of both barcode segments and had unique signatures, such as *Alopias pelagicus* (pelagic thresher), *A. superciliosus* (bigeye thresher) and *Isurus paucus* (longfin mako shark). However, some species displayed probe-barcode hybridisation difficulties (see Methods), with more shark species (7) than ray species (3) being affected, namely *Carcharhinus falciformis* (silky shark), *C. longimanus* (oceanic whitetip shark), *I. oxyrinchus* (shortfin mako shark), *Lamna nasus* (porbeagle shark), *C. brevipinna* (spinner shark), *Galeocerdo cuvier* (tiger shark), *Prionace glauca* (blue shark), *Rhynchobatus laevis* (smoothnose wedgefish), *Glaucostegus typus* (giant shovelnose ray), and *Pristis pristis* (Largetooth sawfish). Nevertheless, some of the species displaying poor probe-barcode hybridisation remained distinguishable using the alternative barcode segment (**Table 1 and Figures S.1-4**).

Based on visual evaluations, the generated melt curves showed different fluorescent signatures for closely related species, such as thresher sharks (*Alopias* spp.) and hammerheads (*Sphyrna* spp.; **Figure 2**). Across the two species of thresher sharks, FASTFISH-ID^{TM} produced visually distinguishable curves in BS1 at the initial stages of the hybridization process and produced a similar drop at ~74-79°C, while the signatures in BS2 were clearly distinct in the initial stages (about 42-47°C). Some species, on the other hand, have virtually identical BS1 signatures but are distinguishable using BS2, such as in the case of zebra shark (*Stegostoma fasciatum*) and spot-tail shark (*C. sorrah*) (**Figure 3**). However, there are problematic

species pairs that have highly similar signatures with both segments and therefore appear visually indistinguishable. This is the case between the tiger shark and giant shovelnose ray, between the silky and blue sharks, and between the giant oceanic manta and giant devil ray (two *Mobula* species), which have nearly identical signatures in both barcode segments (**Figure 4**). Overall, six out of 28 species were deemed visually indistinguishable, four of which are CITES-listed. We also found seven species that amplified inconsistently; shortfin mako shark (*Isurus oxyrinchus*), oceanic whitetip shark (*C. longimanus*), porbeagle shark (*Lamna nasus*), tiger shark (*Galeocerdo cuvier*), largetooth sawfish (*Pristis pristis*), giant shovelnose ray (*Glaucostegus typus*) and smoothnose wedgefish (*Rhynchobatus laevis*). It was observed that the right-most trough in the BS1 fluorescent signature labelled “TM” corresponds to ThermaMark, an internal marker for correction of artefactual temperature variation (**Figure S.5**). However, in BS2, some segments were amplified and unique for each of these species.

Half of the samples were highly processed products, but they still amplified well. In some of these, there were differences in the intensity of the signatures, as reflected in signature variation from BS2 of great hammerhead, zebra shark and bowmouth guitarfish (**Figure 2, 3 and S.4**), which may in part be ascribed to the actual state of degradation of the original DNA template.

Machine learning for species assignment

We transposed data for the training sets and then used fluorescence values at 8,152 temperature intervals (>4,000 per each barcode segment) as variables and identified variable importance as a key feature for species assignment. We ranked variable states according to their relative importance, scaled importance and percentage of variance explained, for each barcode segment (see **Table S.3**)**.** We generated 301 potential deep learning models, aiming for high accuracy and minimizing error. The best deep learning model was chosen as the one with the highest accuracy (98.20%; **Table S.4**). When the model was applied to melt curve data from the independent specimens, accuracy dropped to 79.41%, with 54 out of 68 specimens correctly assigned (**Figure 5**). Mis-assignments were consistent with the species that also proved problematic during visual assessments, i.e. the spinner and blue shark. The model also mis-identified spot-tail shark as zebra shark despite it visually having a

unique signature in BS2 (**Figure 3**). During the testing, some samples from hammerhead sharks (*Sphyrna* spp.), smoothnose wedgefish (*Rhynchobatus laevis*), and broadnose wedgefish (*Rhynchobatus springeri*) were assigned to the wrong species, even though each of these species had their own unique fingerprint (**Figures S.1-4**).

Discussion

Within a couple of hours and without the need to adjust the existing FASTFISH-ID™ assay from teleost fish to elasmobranchs, this real-time PCR method offered a portable monitoring tool that reliably enabled the identification of 25 elasmobranch species (20 of which are CITES-listed). The device used to conduct the runs, the MIC, is a convenient portable real-time PCR thermocycler weighing no more than 2 kg and allowing for the simultaneous inspection of 48 specimens per run (Naaum et al., 2021). More importantly, the use of probes targeting mini barcodes with high inter-specific variation offers a universality that other qPCR-based assays do not currently provide, and the automatic amplification of the full COI barcode as part of the same reaction offers downstream opportunities for further in-depth screening, if necessary.

While existing genetic-based monitoring tools continue to be useful in many situations (Fields et al., 2015; Shivji et al., 2002)(Cardeñosa et al., 2018; Lin et al., 2021), FASTFISH-ID™ seems poised to significantly expand the horizons of DNA-based control: alongside its speed, portability, and universality, the method exhibits single nucleotide resolution (Rice et al., 2014) which can minimize the risk of similar fluorescent signatures, particularly when more species are added to a reference library (Naaum et al., 2021). This is a particularly compelling argument for its implementation, as CITES lists are likely to continue to expand in the future. Additionally, the amplification of the whole COI universal barcode segment embeds a forensic dimension (Dawnay et al., 2007) that is not necessarily afforded by other portable tools.

A difficulty typically encountered in genetic-based trade monitoring is the handling of processed products, and this is particularly true for elasmobranchs which tend to be

heavily processed in a variety of ways (Dharmadi et al., 2019a; Muttaqin et al., 2018). Despite the issues of fragmented DNA due to the effect of various processing techniques (Shokralla et al., 2015), FASTFISH-ID™ shows notable robustness and reliability, with 83.6% of processed samples yielding reliable melt curve profiles (51 of 61 processed samples). Since FASTFISH-ID™ uses real-time PCR and relies on fluorescent signatures, some species display variation in signature amplitude (the variation in peak heights and valley depths) especially when the DNA was degraded, as observed with processed products and displayed by the signature of both hammerhead species on BS2 (**Figure 2**). This deviation may be problematic for species assignment, especially when the assignment depends on a deep learning algorithm. The high probability of the features being similar to those of other species caused misassignments. Other issues that may have occurred is variation in the fluorescence signature from the same species. This could be due to single nucleotide polymorphisms (SNPs) within species or possibly to contamination in the case of the BS2 signature of the pale-edged stingray (*Telatrygon zugei*; **Figure S.4**).

Visual assessment could distinguish 22 species out of 28 with more than half of these (N=17) being CITES-listed. Even in this preliminary phase, the method could therefore readily be applied by inspectors –without the application of computational tools – and reliably reveal cases of illegal activities. Three pairs of species had spectral features that are difficult to distinguish, e.g. these ambiguities were present between tiger shark and giant shovelnose ray, between two species of *Mobula* rays (giant oceanic manta ray and giant devil ray), and between silky and blue shark (**Table 1 - Visual**). Thus, it must be acknowledged that the barcode segments have the same sequence of nucleotides and produced similar signatures for those species. The technology was originally designed for bony fish (Naaum et al., 2021), and the database is currently being expanded to various important species that are globally traded as seafood. Yet, the much lower diversity of elasmobranchs (~1/30th that of teleosts) will make any effort to produce spectral reference databases a far less onerous task than that currently encountered with bony fishes. Whilst it has been known that the COI gene is more slowly evolving in chondrichthyans than teleosts (Moore et al., 2011; Naylor et al., 2012), this is seldom a major issue in most DNA barcoding applications (Fields et al., 2018; Griffiths et al., 2013; Hobbs et al., 2019), so an optimised iteration of the FASTFISH-ID™ method is poised to be

transformational for elasmobranch conservation and management. A qualitative investigation on the full length of COI sequences (Sanger sequencing results) based on visual and simple comparison (https://www.bioinformatics.org/sms2/ident_sim.html) revealed that for those problematic three pairs of species mentioned above for that particular segment, there is a high degree of similarity in their sequence (70-98%), although this seems unlikely as the method is extremely sensitive and easily distinguishes between sequences that differ by a single nucleotide (Sirianni et al., 2016).

In the absence of an online reference database of elasmobranch fluorescent signatures, machine learning was developed for this study. One of the machine learning applications is pattern recognition (Jenrette et al., 2022; Trentin et al., 2018). Deep learning (also known as deep structured learning) is broadly applied in machine learning applications, especially pattern recognition (Jenrette et al., 2022; Trentin et al., 2018) and has advantages in its flexibility to develop learning styles i.e. supervised, semi-supervised or unsupervised (LeCun et al., 2015; Malde et al., 2019). Deep learning models have been chosen and deployed with independent testing datasets to measure their accuracy. We found that the accuracy of our test model was 79.41%, which is lower than the training accuracy (98.20%; **Table S.5**), and yet the model could identify similar species that could not be distinguished visually. In fact, the model enabled us to differentiate the two *Mobula* species that have similar signatures in both barcode segments. Machine learning could also recognize silky shark, a problematic species for the authorities as the species belongs to the Carcharhinidae, a diverse family that has plenty of look-alike species. In particular, the silky shark spectral profiles appeared visually indistinguishable from blue shark. However, the new CITES listing agreed during CoP19 added all requiem sharks into Appendix II (including blue shark along with the other 53 species shark from Carcharhinidae family) will make implementing action manageable since requiem sharks make up a large proportion of the products found in the global shark fin trade hubs in China (Cardeñosa et al., 2022). Although international trade in all requiem sharks will now be regulated, a Non-Detriment Finding (NDF; CITES's mechanism that allows certain species listed in Appendix II to be traded with strict quotas) which is specific to each species will still require the capability of identification at the species level.

Five out of 28 species could not be assigned accurately using the model, i.e. between spot-tail and zebra shark as well as mis-assignments among oceanic whitetip shark, tiger shark and giant shovelnose ray (**Table 1 – Deep Learning**). Curiously, there were also mis-assignments for species that had quite unique fluorescent signatures. We argue that these mis-assignments could be due to variation in amplitude, where some species actually have similar signatures, but different amplitudes (Cusa, 2021) the cause of which is undetermined, but could be due to degraded DNA. For instance, the signature in BS2 of zebra shark has high amplitude variations that may challenge the model to assign the species (**Figure 3**). Increasing training datasets may be required as this should improve the robustness of the model (LeCun et al., 2015), while future re-tailoring of the barcode regions to elasmobranch variation may also remove some of the within-species noise. Despite the assignment problems, when we combine visual and deep learning assignments, we could distinguish 25 out of 28 species, 20 of which are listed in CITES Appendix II.

Limitations of the study

The probe hybridization problems (which occurred when the barcode segments have a high degree of mismatches with the designed probes) encountered in seven species prevented the machine learning tool from adequately assigning fluorescent signatures to a given species. Since BS1 failed to hybridize for most of these species, the species assignment in these cases was solely reliant on BS2, which, in many cases also exhibited poor hybridization. To address this issue, it seems that going forward the designing of new probes tailored to elasmobranch sequence variation will be a necessary solution to increase the versatility and reliability of FASTFISH-ID^{TM}. An increased set of elasmobranch species may also inflate mis-assignments due to the higher degree of similarity among species in both visual-based or machine learning-based systems. There is also limitations in using fully supervised deep learning approaches in the selection of important features from highly variable training sets (e.g. signatures from the two barcode segments) (Hantak et al., 2022). The addition of more species to the database will require more training images. However, with such improvements, this method will help authorities (i.e. fish inspectors, customs and quarantine officers) by providing a single, agile

testing option, at any point in the supply chain, to disentangle the complexity of the shark and ray product trade, and ultimately reduce the consequential risk of extinction for these endangered and iconic taxa.

Acknowledgements

We thank all collaborators of the project Building Capacity to reduce illegal trading of shark products in Indonesia, funded under the Illegal Wildlife Trade (IWT) Challenge Fund number IWT057 and the University of Salford R&E strategy funding, the Ministry for Marine Affairs and Fisheries (MMAF) – Republic of Indonesia, the University of Salford (UoS), the Centre for Environment, Fisheries and Aquaculture Science (Cefas) and the Rekam Nusantara Foundation – Indonesian (REKAM). We also thank the officers and staff of B/LPSPLs ('Balai/Loka Pengelolaan Sumber Daya Pesisir dan Laut'; Institute for Coastal and Marine Resource Management) and Fish Quarantine for helping during field work. We thank staff of the Wildlife Conservation Society – Indonesian Program (WCS-IP) for their support during project initiation. In addition, A.P.P. would personally like to thank Mr. Dharmadi and Dr. Hawis Maddupa for their legacy and supporting the younger generation of scientists seeking to make an impact in conserving elasmobranchs in Indonesia. We also thank Marc Dando for the use of his scientific illustrations of elasmobranchs.

Author contributions

Conceptualization (APP, ADM and SM), Funding acquisition (SM and JMM), Methodology (APP, MC, ADM and SM), Resources (ADM and SM), Investigation (APP and MC), Formal Analysis and Visualization (APP), Project Administration (APP, JMM, FA, ADM and SM), Supervision (ADM and SM), Writing—original draft (APP, ADM and SM), Writing—review & editing (MC, JMM, FA and EM).

Declaration of interests

The authors declare that they have no competing interests.

STAR Methods

Resource availability

Lead contact

Further information and requests for resources and reagents should be directed to and will be fulfilled by the lead contact, Andhika Prasetyo (a.p.prasetyo@edu.salford.ac.uk) or Allan McDevitt (allan.mcdevitt@atu.ie).

Materials availability

This study did not generate new unique reagents. FASTFISH-ID™ reagents were manufactured by Ecologenix, LLC. Natick, MA - USA.

Data and code availability

- Data is archived at the Google Drive and are publicly available of the date of publication database: https://bit.ly/FASTFISH-ID_MS_Supp_Datasets.
- All original code is deposited at the Github repository and are publicly available of the date of publication database: https://github.com/andhikaprima/FastSharkID.
- Any additional information required to reanalyse the data reported in this paper is available from the lead contact upon request.

Experimental model and subject details

Tissue sample of shark and ray specimens were collected in several sites nested in six locations across cities on Java Island, the most populous island in Indonesia (**Figure S.6**, namely Jakarta, Indramayu, Tegal, Cilacap, Surabaya and Banyuwangi. Collected specimens were gathered without prior knowledge of their exact harvest location and were available for collection at a variety of sites, such as fishing ports (FP), traditional markets (TM), processing plants (PP), export hubs (EH) and an inspector station (AU).

Sample collection was granted by research permit no.251/BRSDM/II/2020 issued by Agency for Marine and Fisheries Research and Human Resources AMFRAD, the Ministry of Marine Affairs and Fisheries (MMAF), Republic of Indonesia. Research ethics no. STR1819-45 issued by the Science and Technology Research Ethics

Panel, University of Salford. Export permits no. 00135/SAJI/LN/PRL/IX/2021 (CITES-listed specimens) and 127/LPSPL.2/PRL.430/X/2021 (non-CITES-listed specimens) were granted under the authority of the Ministry of Marine Affairs and Fisheries (MMAF), Republic of Indonesia. Sample were imported into the UK under import permit no. 609191/01-42 from the Animal and Plant Health Agency (APHA), United Kingdom.

Method details

Sample collection and DNA extraction

579 specimens were opportunistically collected at the above-mentioned sites and processing factories throughout January and February 2020. The tissue, which could either be fresh, frozen, partially or heavily processed, was then stored in 2.0mL screw-cap microcentrifuge tubes, submerged in 90% ethanol and stored at 4°C. DNA was extracted from samples following the Mu-DNA protocol for tissue samples (Sellers et al., 2018) with an overnight incubation at 55°C on the thermomixer with a medium mixing frequency and a final elution volume of 100 µl. All surfaces were sterilised with 50% bleach and then washed with 70% ethanol, in-between and after extracting each sample, to reduce cross-contamination risks (**Figure S.7a-b)**.

Of these, we excluded specimens of unclear taxonomy, and all species represented by less than 3 individuals. We refined the collection to 130 tissue samples (specimens) belonging to 28 species; for each species, we used three replicates per specimen as training sets (390 runs) (**Table S.1)**. We also had another 68 tissue samples without replication and used them as testing datasets (**Table S.2)**. As sampling was conducted opportunistically, we did not have an equal number of samples per species. Some species had a limited number of specimens, so we took out some training sets to be used as testing datasets. Datasets were then filtered, and ambiguous qPCR runs (i.e. poor probe-barcode hybridisation or inconsistent fluorescent signature) were removed. A poor probe-barcode hybridisation was checked using a reference point created by ThermaMark^{TM} (TM) in the signature produced from BS1. If only ThermaMark^{TM} (TM) amplified in the BS1 fluorescent signature, those runs would have failed to hybridize. Inconsistent fluorescent signatures within a replication or species were re-run a second time. If the re-runs kept failing, those runs were removed. In the end, we used 357 (number of

replications varied by specimens) and 68 runs for training and testing datasets, respectively.

FASTFISH-ID™ closed-tube barcoding protocol

PCR reaction and amplification conditions

In the first instance, the FASTFISH-ID™ method requires the amplification of the full cytochrome c oxidase I (COI) gene (~650 bp) and in the second instance, it targets the two mini-barcodes (~80 bp) using a set of probes. PCR master mixes were prepared in low-adhesion Eppendorf tubes (Naaum et al., 2021). The major components of this method are ThermaStop™, ThermaMark™ and FASTFISH-ID™ Probe Mix (Ecologenix, LLC.). ThermaStop™ is a novel hot-start reagent that prevents non-specific amplification prior to the start of the reaction, while ThermaMark™ (hereafter referred as TM) is a temperature-dependent marker for correction of melt-curve analysis (Ecologenix, LLC.). The FASTFISH-ID™ probe mix consisted of two sets of positive/negative probe pairs labelled in two different colours that hybridize along the length of two mini-barcode regions within the amplified COI target sequence, hereafter referred to as Barcoding Segment 1 (BS1) and Barcoding Segment 2 (BS2). A M13 primer was used as a priming site that facilitates the sequencing process for eventual species validation through Sanger sequencing.

FASTFISH-ID™ uses asymmetric PCR to produce more single stranded amplicons which allow the probes to hybridize more easily (Sanchez et al., 2004). After amplification, mismatch tolerant positive/negative probe pairs bind to their single-stranded DNA targets. Each positive-probe is formed of a target binding sequence that is 20–35 nucleotides long and has a higher fluorescent signal when it is bound to its target sequence but a low background fluorescence when it is not. Negative-probes are only quenchers that reduce the fluorescent signal when they are bound next to their paired positive-probe. Positive/negative probe pairs can bind to both perfectly matching strands and target sequence variants with one or more nucleotide polymorphisms. This means that they can tolerate mismatches, which is one of the most important features of this technology as a single set of reagents can be used to identify a large number of species (Naaum et al., 2021). Target sequences that are similar but different, even if only by one nucleotide, almost always have different fluorescent signatures. Positive/negative probe sets therefore have the potential to

discriminate among thousands of fish species and their variants (Naaum et al., 2021).

PCR amplification was performed on a Magnetic Induction Cycler (MIC) which is a real-time PCR thermocycler designed by Bio Molecular Systems™ (Upper Coomera, Queensland, Australia). Thermocycling conditions were 94°C for 2 mins, 5 cycles of 94°C for 5 secs, 55°C for 20 secs, 72°C for 45 secs, then 65 cycles of 94°C for 5 secs, 70°C for 45 secs (in total: 2 hrs, 20 mins and 44 secs). Following a total of 70 amplification cycles, the reaction leads to a 10- to 20-fold excess of single-stranded DNA which is critical for probe/target hybridization in a single closed tube (Pierce et al., 2005; Sanchez et al., 2004). At the completion of PCR, the temperature was decreased down to 40°C for 10 mins to enable the fluorescent probes in the FASTFISH-ID™ probe mix to hybridize to the excess single-stranded DNA. This step was followed by a melting curve analysis where the temperature was gradually increased from 40°C to 87°C at 0.1°C /secs with sequential fluorescent acquisition first in the MIC PCR Cycler's Orange Channel (suitable for detection of CalRed 610-labelled probes; max excitation: 590 nm; max emission 610 nm) and then detection in the Red Channel (suitable for detection of Quasar 670-labelled probes; max excitation: 647 nm; max emission 670 nm). The first derivative of the melt curve was then used as the fluorescent signature. Species assignment was revealed by comparing a distinct mix of Cal-Red 610 and Quasar 670 fluorescent signatures (**Figure S.7c-f**). Those multiple combinations allow FASTFISH-ID™ to identify a large number of species with the same reagents (Naaum et al., 2021; Rice et al., 2012; Sirianni et al., 2016).

DNA barcoding and species validation

The same single strand DNA products used to generate a fluorescent signature can also be sequenced by DNA barcoding for further investigation. The sequencing protocol uses the M13 tail sequence in the FASTFISH-ID™ FISH COI HBCts excess primer (5' CACGACGTTGTAAAACGAC 3', a modified version of the M13F primer) as a sequencing primer to generate the sequence of the excess primer strand. By design, the excess primer-strand sequence can be queried directly in the NCBI nucleotide database (NCBI, 1988) or the Barcode of Life Database (Ratnasingham and Hebert, 2007) for species identification. In addition, we also used Fish F2 (5'

TCGACTAATCATAAAGATATCGGCAC 3') and Fish R2 (5′ ACTTCAGGGTGACCGAAGAATCAGAA 3′) primer sets (Ward et al., 2005) for several initial specimens for comparison with HBCts excess primer (M13). Sequencing was outsourced to Macrogen Europe™. Samples were prepared according to the service provider protocols (https://www.macrogen-europe.com/services/sanger-sequencing). We also added species and/or specimens after identification using a highly degenerated primer set using a high throughput barcoding (HTB) method (A.P. Prasetyo et al., *unpublished data*); Leray-XT primer sets (313 bp). This set included the primers jgHCO2198 (5′ TAIACYTCIGGRTGICCRAARAAYCA 3′) and mlCOIintF-XT (5′ GGWACWRGWTGRACWITITAYCCYCC 3′) (Wangensteen et al., 2018).

Quantification and statistical analysis

Machine learning for species assignment

Since the two probing barcode segments and the algorithm were developed for teleost fishes, they are not expected to maximise differentiation among the melt curves of elasmobranch species. Furthermore, the existing cloud-based reference library does not contain any elasmobranch signatures. We therefore developed our own species identification system by using machine learning using the H2O platform (**Figure S.7h-g)**. H2O is an open source, fast and scalable machine learning and predictive analytics platform that allows building machine learning models on big data, and improving reproducibility (Candel et al., 2016). The deep learning algorithm was deployed to address the problem of species assignment by considering its capability to arrange multiple nonlinear transformations to model high-level abstractions in data. H2O's Deep Learning is based on a multi-layer feedforward artificial neural network (FANN) that is trained with a stochastic gradient descent using a backpropagation environment (Candel et al., 2016). Deep learning is also advantaged by extracting the optimal input representation from raw data without user intervention (Avci et al., 2021).

The fluorescent signature datasets (BS1 and BS2) were extracted, with the species identity serving as the "response", and the transposed PCR profile temperature values being used as the predictor "variables" (each barcode fragment is recorded at about 4,000 temperature values), and fluorescent values serving as the "feature". In

deep learning, “response” refers to the individual value that served as the output (species name in our case); while “variable” refers to properties of the “response” and is evaluated through the “feature”.

The performance of deep learning algorithms depends heavily on the extracted features, so it's important to choose the right group of features that best represent the input data (Pouyanfar et al., 2018). Data filtering was conducted to exclude poor probe-barcode hybridisation or inconsistent fluorescent signature datasets and provided the best representative of the data input. Two datasets (BS1 and BS2) were then merged by specimen ID with species name used as an input to the model. Our model was divided using a 70–30 ratio of training data to validation data (i.e. 246 and 111 runs respectively) and then tested with 68 independent datasets. Default parameters of H2O’s Deep Learning were optimized, with a process called “grid-search”, this process tried to adjust several parameters to find the optimal “stopping criteria” (list of parameters provided on **Table S.6**). We setup a “stopping criteria” to limit the computational load in searching for the best deep learning algorithm, which was based on random discreteness, the number of generated models, and model runtime (**Table S.7**). The best model was chosen based on model accuracy and Root Mean Square Error (RMSE) optimization. A confusion matrix is used to visualize model accuracy.

As for other algorithms, larger databases are required to improve predictive abilities by optimizing distributed representation, activation function non-linearity, and flexible architecture depth in terms of hidden layers and nodes (Calzolari and Liu, 2021). The main challenges in applying deep learning is overfitting due to a dominant influence on the generalization ability of a deep neural network model (Li et al., 2019). However, regularization methods such as Ivakhnenko's unit pruning (Ivakhnenko, 1971) or sparsity (l_1-regularization) or weight decay (l_2-regularization) can be applied during training to combat overfitting (Bengio et al., 2013). The sparsity and weight decay were used in this study.

Key resources table

REAGENT or RESOURCE	SOURCE	IDENTIFIER
Biological samples		
198 tissue samples (specimens) belonging to 28 species	This paper	https://www.ncbi.nlm.nih.gov/sra/?term=PRJNA850687
Chemicals		
Mu-DNA extraction reagents	(Sellers et al., 2018)	https://www.protocols.io/view/mu-dna-a-modular-universal-dna-extraction-method-a-6gpvryj2gmkn/v2
Commercial assays		
FASTFISH-ID™ Probe Mix	Ecologenix, LLC. Natick, MA - USA	https://www.fastspecies-id.com/
Deposited data		
Training and testing datasets	This paper	
Software and algorithms		
H2O	H2O.ai	https://h2o.ai/platform/ai-cloud/make/h2o/
pandas	The pandas development team	Libraryhttps://pandas.pydata.org
Deep learning algorithm for species recognition	This paper	https://github.com/andhikaprima/FastSharkID
Oligonucleotides		
M13F primer	Macrogen™	Ecologenix, LLC. Natick, MA - USA
Fish02 primer sets	Macrogen™	(Ward et al., 2005)
Leray-XT primer sets	Macrogen™	(Wangensteen et al., 2018)

References

Ali, A., Fahmi, Dharmadi, Krajangdara, T., and Khiok, A.L.P. (2018). Biodiveristy and habitat preferences of living sharks in the Southeast Asian Region. Indonesia Fisheries Research Journal *24*, pp. 133-140. doi: 10.15578/ifrj.24.2.2018.133-140.

Ali, A., Khiok, A.L.P., Fahmi, Dharmadi, and Krajangdara, T. (2014). Field guide to Rays, Skates and Chimaeras of the Southeast Asian Region (SEAFDEC). doi.

Avci, O., Abdeljaber, O., Kiranyaz, S., Hussein, M., Gabbouj, M., and Inman, D.J. (2021). A review of vibration-based damage detection in civil structures: From traditional methods to Machine Learning and Deep Learning applications. Mechanical Systems and Signal Processing *147*, pp. 107077. doi: 10.1016/j.ymssp.2020.107077.

605 Bar-On, Y.M., Phillips, R., and Milo, R. (2018). The biomass distribution on Earth.
606 Proceedings of the National Academy of Sciences *115*, pp. 6506-6511. doi:
607 10.1073/pnas.1711842115.
608 Bengio, Y., Boulanger-Lewandowski, N., and Pascanu, R. (2013). Advances in
609 optimizing recurrent networks. 26-31 May 2013. pp. 8624-8628.
610 Booth, H., Muttaqin, E., Simeon, B., Ichsan, M., Siregar, U., Yulianto, I., and Kassem,
611 K. (2018). Shark and ray conservation and management in Indonesia: Status
612 and strategic priorities 2018-2023. Wildlife Conservation Society.
613 Calzolari, G., and Liu, W. (2021). Deep learning to replace, improve, or aid CFD
614 analysis in built environment applications: A review. Building and Environment
615 *206*, pp. 108315. doi: 10.1016/j.buildenv.2021.108315.
616 Candel, A., Parmar, V., LeDell, E., and Arora, A. (2016). Deep learning with H2O.
617 H2O. ai Inc, pp. 1-21. doi.
618 Cardeñosa, D., Quinlan, J., Shea, K.H., and Chapman, D.D. (2018). Multiplex real-
619 time PCR assay to detect illegal trade of CITES-listed shark species. Scientific
620 Reports *8*, pp. 16313. doi: 10.1038/s41598-018-34663-6.
621 Cardeñosa, D., Shea, S.K., Zhang, H., Fischer, G.A., Simpfendorfer, C.A., and
622 Chapman, D.D. (2022). Two thirds of species in a global shark fin trade hub
623 are threatened with extinction: Conservation potential of international trade
624 regulations for coastal sharks. Conservation Letters *n/a*, pp. e12910. doi:
625 10.1111/conl.12910.
626 Cawthorn, D.-M., and Mariani, S. (2017). Global trade statistics lack granularity to
627 inform traceability and management of diverse and high-value fishes.
628 Scientific Reports *7*, pp. 12852. doi: 10.1038/s41598-017-12301-x.
629 CITES (2022). 19.218 - 19.225 Sharks and rays (Elasmobranchii spp.). CITES.
630 Clarke, S.C., McAllister, M.K., Milner-Gulland, E.J., Kirkwood, G.P., Michielsens,
631 C.G.J., Agnew, D.J., Pikitch, E.K., Nakano, H., and Shivji, M.S. (2006). Global
632 estimates of shark catches using trade records from commercial markets.
633 Ecology Letters *9*, pp. 1115–1126. doi: 10.1111/j.1461-0248.2006.00968.x.
634 Collyns, D. (2022). Shark fin trade regulated at last in landmark decision. Wildlife.
635 Published online 18 Nov 2022 doi.
636 Cusa, M. (2021). Towards improved traceability in the seafood industry. Doctor of
637 Philosophy (PhD) (University of Salford).

638 Dawnay, N., Ogden, R., McEwing, R., Carvalho, G.R., and Thorpe, R.S. (2007).
639 Validation of the barcoding gene COI for use in forensic genetic species
640 identification. Forensic Science International *173*, pp. 1-6. doi:
641 10.1016/j.forsciint.2006.09.013.
642 Dent, F., and Clarke, S. (2015). State of the global market for shark products (Food
643 and Agriculture Organization of the United Nations). doi.
644 Dharmadi, Fahmi, and Satria, F. (2015). Fisheries management and conservation of
645 sharks in Indonesia. African Journal of Marine Science *37*, pp. 249–258. doi:
646 10.2989/1814232X.2015.1044908.
647 Dharmadi, Prasetyo, A., and Ahmad, A. (2019a). Marketing and Trade of Sharks and
648 Rays in Java and Sumatera (Indonesia). SEAFDEC/MFRDMD.
649 http://opac.seafdec.org.my/handle/20.500.12561/800.
650 Dharmadi, Prasetyo, A.P., and Ali, A. (2019b). Marketing and Trade of S&R in Java
651 and Sumatera, Indonesia. SEAFDEC/MFRDMD.
652 Dulvy, N.K., Fowler, S.L., Musick, J.A., Cavanagh, R.D., Kyne, P.M., Harrison, L.R.,
653 Carlson, J.K., Davidson, L.N.K., Fordham, S.V., Francis, M.P., et al. (2014).
654 Extinction risk and conservation of the world's sharks and rays. eLife *3*, pp. 1-
655 34. doi.
656 Fahmi, and Dharmadi (2015). Pelagic shark fisheries of Indonesia's Eastern Indian
657 Ocean Fisheries Management Region. African Journal of Marine Science *37*,
658 pp. 259-265. doi: 10.2989/1814232X.2015.1044908.
659 FAO (2021). Fishery and Aquaculture Statistics. Global Fish Trade - All partners
660 aggregated 1976-2019 (FishstatJ). FAO Fisheries and Aquaculture Division
661 [online]. doi.
662 FAO (2022). Fishery and Aquaculture Statistics. Global capture production 1950-2020
663 (FishStatJ). In: FAO Fisheries and Aquaculture Division [online].
664 Fields, A.T., Abercrombie, D.L., Eng, R., Feldheim, K., and Chapman, D.D. (2015). A
665 Novel Mini-DNA Barcoding Assay to Identify Processed Fins from
666 Internationally Protected Shark Species. PLOS ONE *10*, pp. e0114844. doi:
667 10.1371/journal.pone.0114844.
668 Fields, A.T., Fischer, G.A., Shea, S.K.H., Zhang, H., Abercrombie, D.L., Feldheim,
669 K.A., Babcock, E.A., and Chapman, D.D. (2018). Species composition of the
670 international shark fin trade assessed through a retail-market survey in Hong
671 Kong. Conservation Biology *32*, pp. 376-389. doi: 10.1111/cobi.13043.

672 Garcia, R., Prados, R., Quintana, J., Tempelaar, A., Gracias, N., Rosen, S., Vågstøl,
673 H., and Løvall, K. (2019). Automatic segmentation of fish using deep learning
674 with application to fish size measurement. ICES Journal of Marine Science *77*,
675 pp. 1354-1366. doi: 10.1093/icesjms/fsz186.
676 Griffiths, A.M., Miller, D.D., Egan, A., Fox, J., Greenfield, A., and Mariani, S. (2013).
677 DNA barcoding unveils skate (Chondrichthyes: Rajidae) species diversity in
678 'ray' products sold across Ireland and the UK. PeerJ *1*, pp. e129. doi:
679 10.7717/peerj.129.
680 Hantak, M.M., Guralnick, R.P., Zare, A., and Stucky, B.J. (2022). Computer vision for
681 assessing species color pattern variation from web-based community science
682 images. iScience *25*. doi: 10.1016/j.isci.2022.104784.
683 Hobbs, C.A.D., Potts, R.W.A., Bjerregaard Walsh, M., Usher, J., and Griffiths, A.M.
684 (2019). Using DNA Barcoding to Investigate Patterns of Species Utilisation in
685 UK Shark Products Reveals Threatened Species on Sale. Scientific Reports
686 *9*, pp. 1028. doi: 10.1038/s41598-018-38270-3.
687 Ivakhnenko, A.G. (1971). Polynomial Theory of Complex Systems. IEEE Transactions
688 on Systems, Man, and Cybernetics *SMC-1*, pp. 364-378. doi:
689 10.1109/TSMC.1971.4308320.
690 Jenrette, J., Liu, Z.Y.C., Chimote, P., Hastie, T., Fox, E., and Ferretti, F. (2022). Shark
691 detection and classification with machine learning. Ecological Informatics *69*,
692 pp. 101673. doi: 10.1016/j.ecoinf.2022.101673.
693 LeCun, Y., Bengio, Y., and Hinton, G. (2015). Deep learning. Nature *521*, pp. 436-444.
694 doi: 10.1038/nature14539.
695 Leung, B., Hargreaves, A.L., Greenberg, D.A., McGill, B., Dornelas, M., and Freeman,
696 R. (2020). Clustered versus catastrophic global vertebrate declines. Nature
697 *588*, pp. 267-271. doi: 10.1038/s41586-020-2920-6.
698 Li, H., Li, J., Guan, X., Liang, B., Lai, Y., and Luo, X. (2019). Research on Overfitting
699 of Deep Learning. 13-16 Dec. 2019. pp. 78-81.
700 Lin, T.-C., Hsiao, W.V., Han, S.-J., Joung, S.-J., and Shiao, J.-C. (2021). A direct
701 multiplex loop-mediated isothermal amplification method to detect three
702 CITES-listed shark species. Aquatic Conservation: Marine and Freshwater
703 Ecosystems *31*, pp. 2193-2203. doi: 10.1002/aqc.3592.
704 MacNeil, M.A., Chapman, D.D., Heupel, M., Simpfendorfer, C.A., Heithaus, M.,
705 Meekan, M., Harvey, E., Goetze, J., Kiszka, J., Bond, M.E., et al. (2020).

706 Global status and conservation potential of reef sharks. Nature *583*, pp. 801-
707 806. doi: 10.1038/s41586-020-2519-y.
708 Malde, K., Handegard, N.O., Eikvil, L., and Salberg, A.-B. (2019). Machine intelligence
709 and the data-driven future of marine science. ICES Journal of Marine Science
710 *77*, pp. 1274-1285. doi: 10.1093/icesjms/fsz057.
711 Mardhiah, U., Booth, H., Simeon, B.M., Muttaqin, E., Ichsan, M., Dharmadi, Fahmi,
712 Prasetyo, A.P., and Yulianto, I. (2019). Quantifying vulnerability of sharks and
713 rays species in Indonesia: Is biological knowledge sufficient enough for the
714 assessment? IOP Conference Series: Earth and Environmental Science *278*,
715 pp. 012043. doi: 10.1088/1755-1315/278/1/012043.
716 Moore, A.B.M., White, W.T., Ward, R.D., Naylor, G.J.P., and Peirce, R. (2011).
717 Rediscovery and redescription of the smoothtooth blacktip shark,
718 *Carcharhinus leiodon* (Carcharhinidae), from Kuwait, with notes on its possible
719 conservation status. Marine and Freshwater Research *62*, pp. 528-539. doi:
720 10.1071/MF10159.
721 Muttaqin, E., Simeon, B., Ichsan, M., Dharmadi, Prasetyo, A.P., Booth, H., Yulianto,
722 I., and Friedman, K. (2018). The Scalem Value and Importance of Non-fin
723 Shark and Ray Commodities in Indonesia. Food and Agriculture Organization
724 of the United Nations; Ministry of Marine Affairs and Fisheries; and Wildlife
725 Conservation Society.
726 Naaum, A., and Hanner, R. (2016). Seafood traceability and authenticity: A DNA-base
727 d perspective. USA: Academic Press.
728 Naaum, A.M., Cusa, M., Singh, M., Bleicher, Z., Elliott, C., Goodhead, I.B., Hanner,
729 R.H., Helyar, S.J., Mariani, S., Rice, J.E., et al. (2021). Validation of
730 FASTFISH-ID: A new commercial platform for rapid fish species
731 authentication via universal closed-tube barcoding. Food Research
732 International *141*, pp. 110035. doi: 10.1016/j.foodres.2020.110035.
733 Naylor, G.J.P., Caira, J.N., Jensen, K., Rosana, K.A.M., White, W.T., and Last, P.R.
734 (2012). A DNA Sequence–Based Approach To the Identification of Shark and
735 Ray Species and Its Implications for Global Elasmobranch Diversity and
736 Parasitology. Bulletin of the American Museum of Natural History *2012*, pp. 1-
737 262. doi.
738 NCBI (1988). Nucleotide [Internet]. Bethesda (MD): National Library of Medicine,
739 National Center for Biotechnology Information.

740 Nugraha, B., Prasetyo, A.P., Mahiswara, Sianipar, A.B., Canisthya, E., Gautama, D.A.,
741 Ramadhani, R., Muttaqin, E., Ichsan, M., Simeon, B., et al. (2020). Pedoman
742 Pendataan Perikanan Hiu dan Pari di Lokasi Pendaratan (Kementerian
743 Kelautan dan Perikanan). doi.
744 Oktaviyani, S., Simeon, B., Dharmadi, Prasetyo, A.P., Sudarisman, R., Prabowo,
745 Muttaqin, E., Setiono, Ichsan, M., Sari, R.P., et al. (2019). Panduan
746 penyusunan non-detriment findings (NDF) untuk jenis hiu di indonesia (Media
747 Sains Nasional). doi: 10.13140/RG.2.2.22504.21767.
748 Pacoureau, N., Rigby, C.L., Kyne, P.M., Sherley, R.B., Winker, H., Carlson, J.K.,
749 Fordham, S.V., Barreto, R., Fernando, D., Francis, M.P., et al. (2021). Half a
750 century of global decline in oceanic sharks and rays. Nature *589*, pp. 567-571.
751 doi: 10.1038/s41586-020-03173-9.
752 Pavitt, A., Malsch, K., King, E., Chevalier, A., Kachelriess, D., Vannuccini, S., and
753 Friedman, K. (2021). CITES and the sea: Trade in commercially exploited
754 CITES-listed marine species. FAO.
755 Peña, A., Pérez, N., Benítez, D.S., and Hearn, A. (2021). Hammerhead Shark Species
756 Monitoring with Deep Learning. held in Cham, 2021//. A.D. Orjuela-Cañón, J.
757 Lopez, J.D. Arias-Londoño, and J.C. Figueroa-García, eds. (Springer
758 International Publishing), pp. 45-59.
759 Pierce, K.E., Sanchez, J.A., Rice, J.E., and Wangh, L.J. (2005). Linear-After-The-
760 Exponential (LATE)-PCR: Primer design criteria for high yields of specific
761 single-stranded DNA and improved real-time detection. Proceedings of the
762 National Academy of Sciences *102*, pp. 8609-8614. doi:
763 10.1073/pnas.0501946102.
764 Pouyanfar, S., Sadiq, S., Yan, Y., Tian, H., Tao, Y., Reyes, M.P., Shyu, M.-L., Chen,
765 S.-C., and Iyengar, S.S. (2018). A survey on deep learning: Algorithms,
766 techniques, and applications. ACM Computing Surveys (CSUR) *51*, pp. 1-36.
767 doi: 10.1145/3234150.
768 Prasetyo, A.P., McDevitt, A.D., Murray, J.M., Barry, J., Agung, F., Muttaqin, E., and
769 Mariani, S. (2021). Shark and ray trade in and out of Indonesia: Addressing
770 knowledge gaps on the path to sustainability. Marine Policy *133*, pp. 104714.
771 doi: 10.1016/j.marpol.2021.104714.

772 Ratnasingham, S., and Hebert, P.D.N. (2007). bold: The Barcode of Life Data System
773 (http://www.barcodinglife.org). Molecular Ecology Notes *7*, pp. 355-364. doi:
774 10.1111/j.1471-8286.2007.01678.x.
775 Rice, J.E., Reis Jr, A.H., Rice, L.M., Carver-Brown, R.K., and Wangh, L.J. (2012).
776 Fluorescent signatures for variable DNA sequences. Nucleic Acids Res *40*,
777 pp. e164-e164. doi.
778 Safari, E., and Hassan, Z.-M. (2020). Immunomodulatory effects of shark cartilage:
779 Stimulatory or anti-inflammatory. Process Biochemistry *92*, pp. 417-425. doi:
780 10.1016/j.procbio.2020.01.032.
781 Sanchez, J.A., Pierce, K.E., Rice, J.E., and Wangh, L.J. (2004). Linear-After-The-
782 Exponential (LATE)-PCR: An advanced method of asymmetric PCR and its
783 uses in quantitative real-time analysis. Proceedings of the National Academy
784 of Sciences *101*, pp. 1933-1938. doi: 10.1073/pnas.0305476101.
785 Sellers, G.S., Muri, C.D., Gómez, A., and ing, B.H.n. (2018). Mu-DNA: a modular
786 universal DNA extraction method adaptable for a wide range of sample types.
787 Metabarcoding and Metagenomics *2*, pp. e24556. doi:
788 10.3897/mbmg.2.24556.
789 Sharma, N., Scully-Power, P., and Blumenstein, M. (2018). Shark Detection from
790 Aerial Imagery Using Region-Based CNN, a Study. held in Cham, 2018//. T.
791 Mitrovic, B. Xue, and X. Li, eds. (Springer International Publishing), pp. 224-
792 236.
793 Shea, K.H., and To, A.W.L. (2017). From boat to bowl: Patterns and dynamics of shark
794 fin trade in Hong Kong — implications for monitoring and management. Marine
795 Policy *81*, pp. 10. doi: 10.1016/j.marpol.2017.04.016.
796 Shivji, M., Clarke, S., Pank, M., Natanson, L., Kohler, N., and Stanhope, M. (2002).
797 Genetic Identification of Pelagic Shark Body Parts for Conservation and Trade
798 Monitoring. Conservation Biology *16*, pp. 1036-1047. doi.
799 Shokralla, S., Hellberg, R.S., Handy, S.M., King, I., and Hajibabaei, M. (2015). A DNA
800 Mini-Barcoding System for Authentication of Processed Fish Products.
801 Scientific Reports *5*, pp. 15894. doi: 10.1038/srep15894.
802 Simpfendorfer, C.A., and Dulvy, N.K. (2017). Bright spots of sustainable shark fishing.
803 Current Biology *27*, pp. R97-R98. doi: 10.1016/j.cub.2016.12.017.

804 Sirianni, N.M., Yuan, H., Rice, J.E., Kaufman, R.S., Deng, J., Fulton, C., Wangh, L.J.,
805 and Steinke, D. (2016). Closed-Tube Barcoding. Genome *59*, pp. 1049-1061.
806 doi: 10.1139/gen-2016-0026.
807 Trentin, E., Schwenker, F., El Gayar, N., and Abbas, H.M. (2018). Off the Mainstream:
808 Advances in Neural Networks and Machine Learning for Pattern Recognition.
809 Neural Processing Letters *48*, pp. 643-648. doi: 10.1007/s11063-018-9830-8.
810 Wangensteen, O.S., Palacín, C., Guardiola, M., and Turon, X. (2018). DNA
811 metabarcoding of littoral hard-bottom communities: high diversity and
812 database gaps revealed by two molecular markers. PeerJ *6*, pp. e4705. doi:
813 10.7717/peerj.4705.
814 Ward, R.D., Zemlak, T.S., Innes, B.H., Last, P.R., and Hebert, P.D.N. (2005). DNA
815 barcoding Australia's fish species. Philosophical Transactions of the Royal
816 Society B: Biological Sciences *360*, pp. 1847-1857. doi:
817 10.1098/rstb.2005.1716.
818

Figures

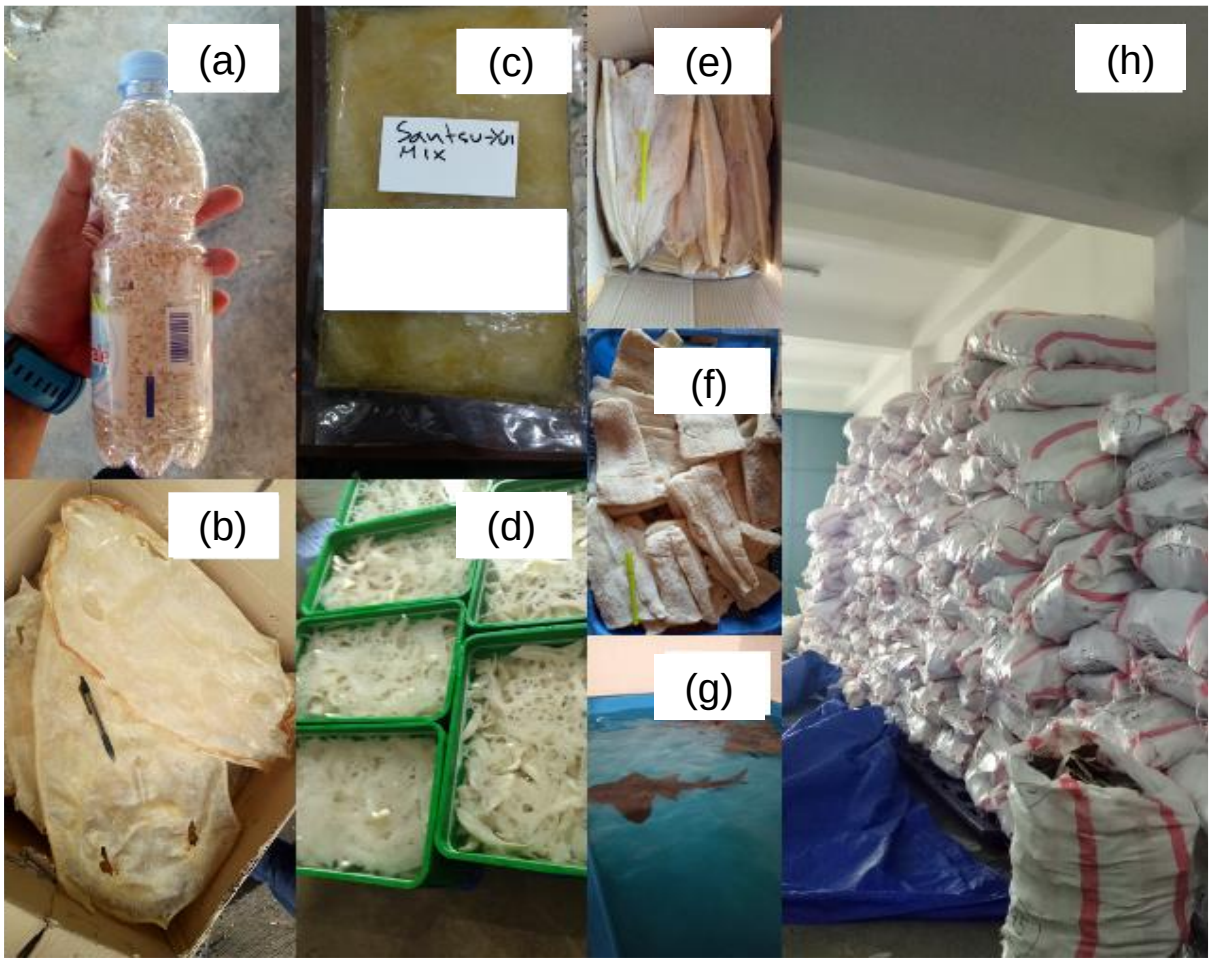

Figure 1. Condition of inspection and some derivative products from sharks and rays i.e. shark teeth (a); processed ray skin (b); shredded fins 'hissit' in brine ready for exporting to Japan (c); blue shark cartilages soaked for processing (d); dried meat from small sharks (e); dried meat from a large shark (f); live bowmouth guitarfish for the aquarium market (g); and dried fins of silky and hammerhead sharks waiting for quota to export (h).

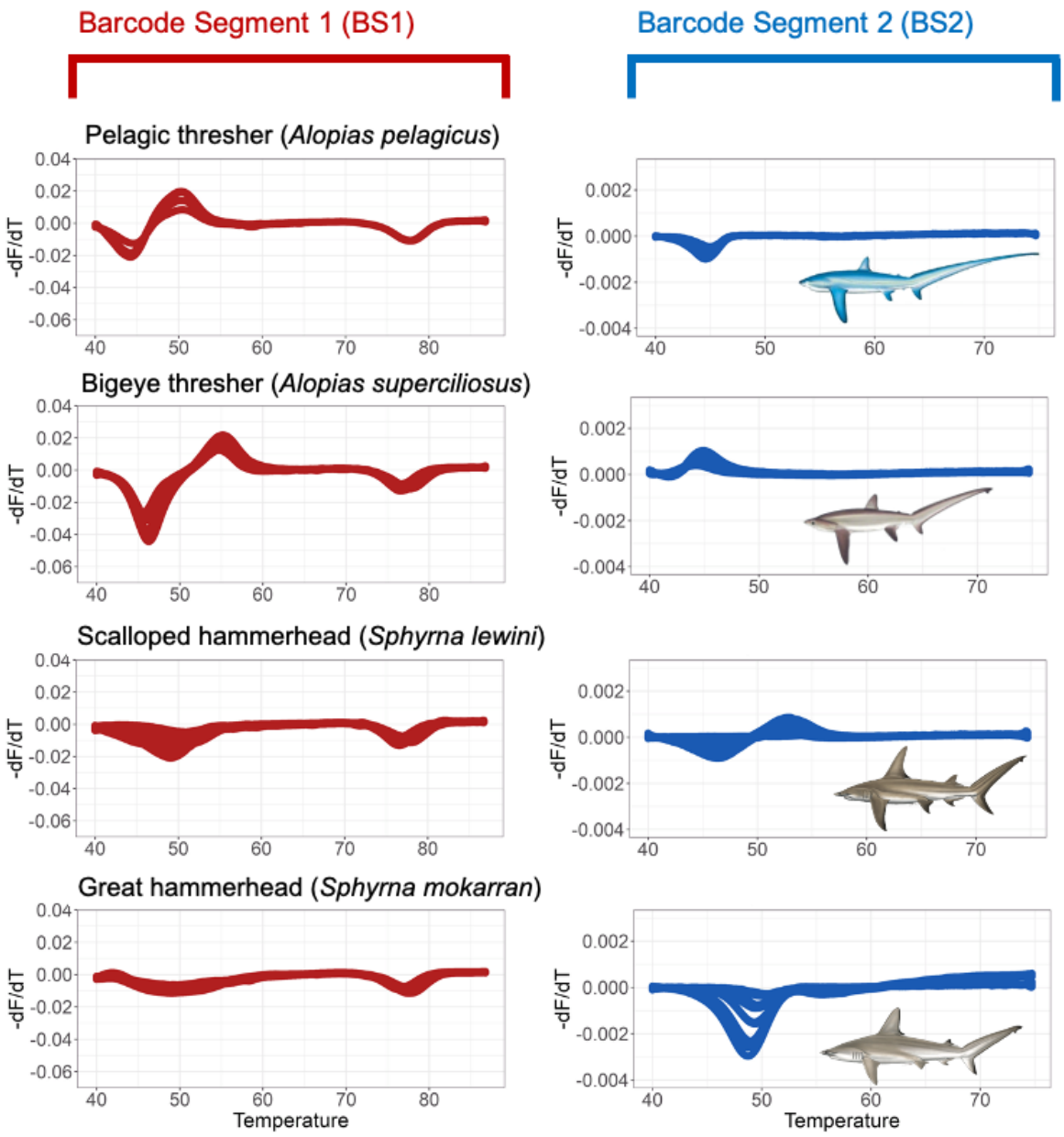

Figure 2. Some species that have visually distinguishable signatures in both barcode segments i.e. pelagic thresher, bigeye thresher, scalloped hammerhead and great hammerhead.

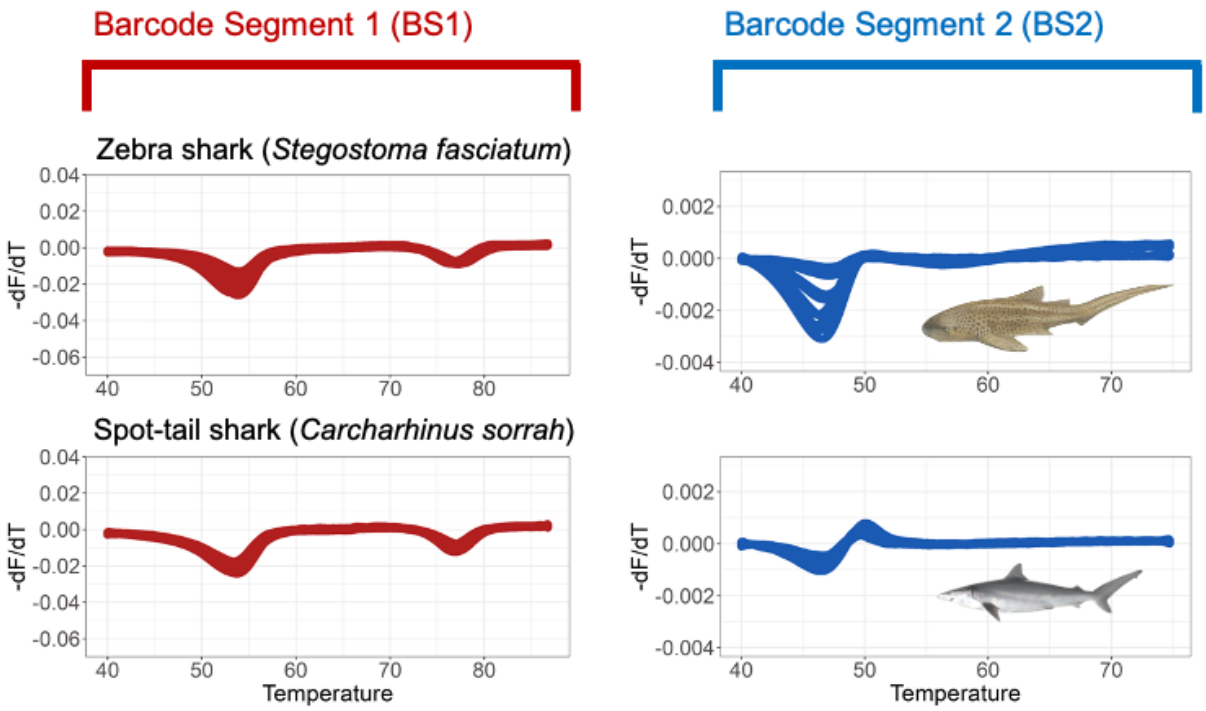

Figure 3. Some species that have similar signature in one barcode segment but visually unique in other segment i.e. zebra and spot-tail shark.

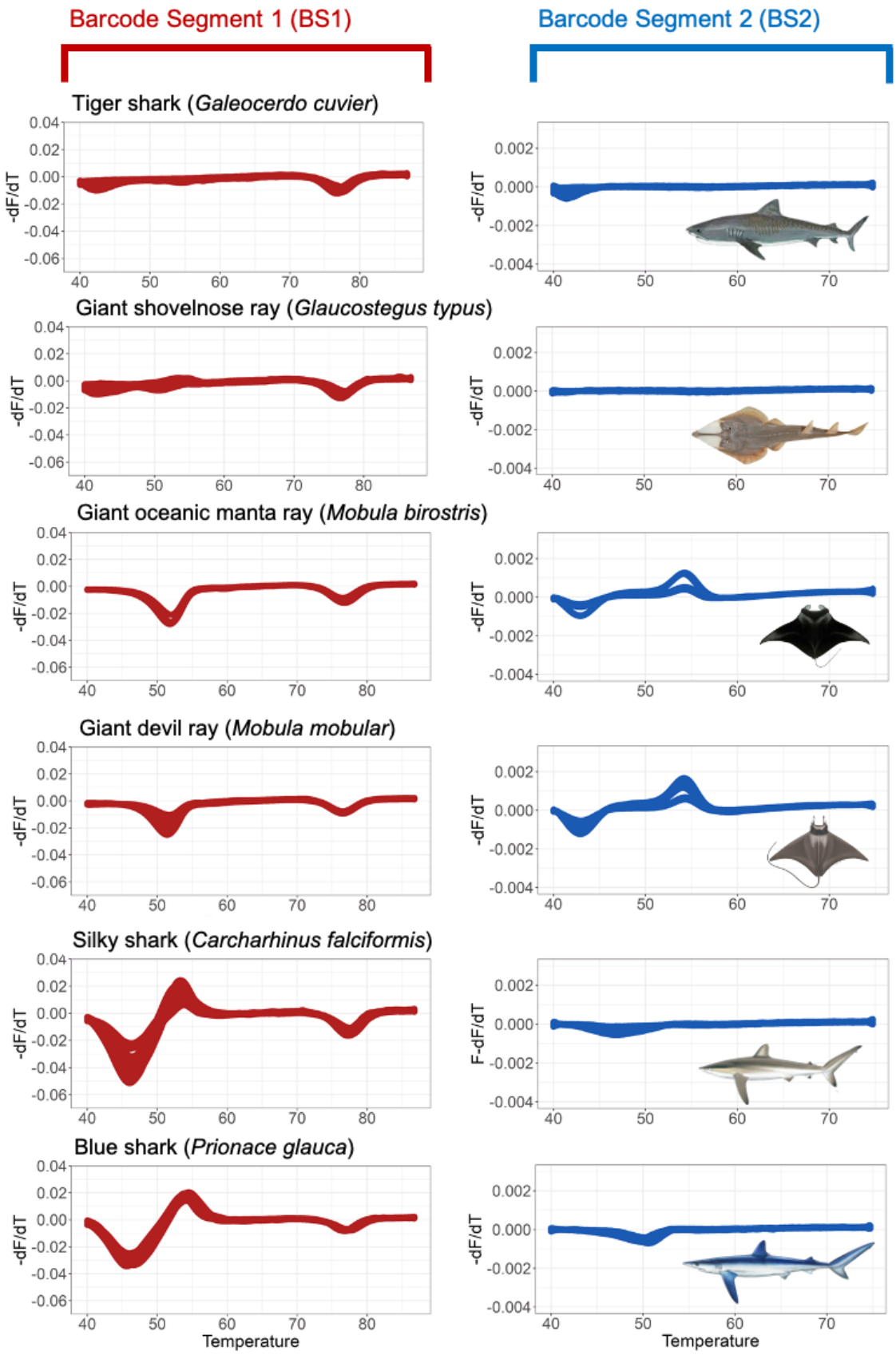

838
839 **Figure 4.** Problematic species that visually have highly similar signatures at
840 both barcode segments i.e. tiger shark and giant shovelnose ray; giant
841 oceanic manta ray and giant devil ray; silky shark and blue shark.

842

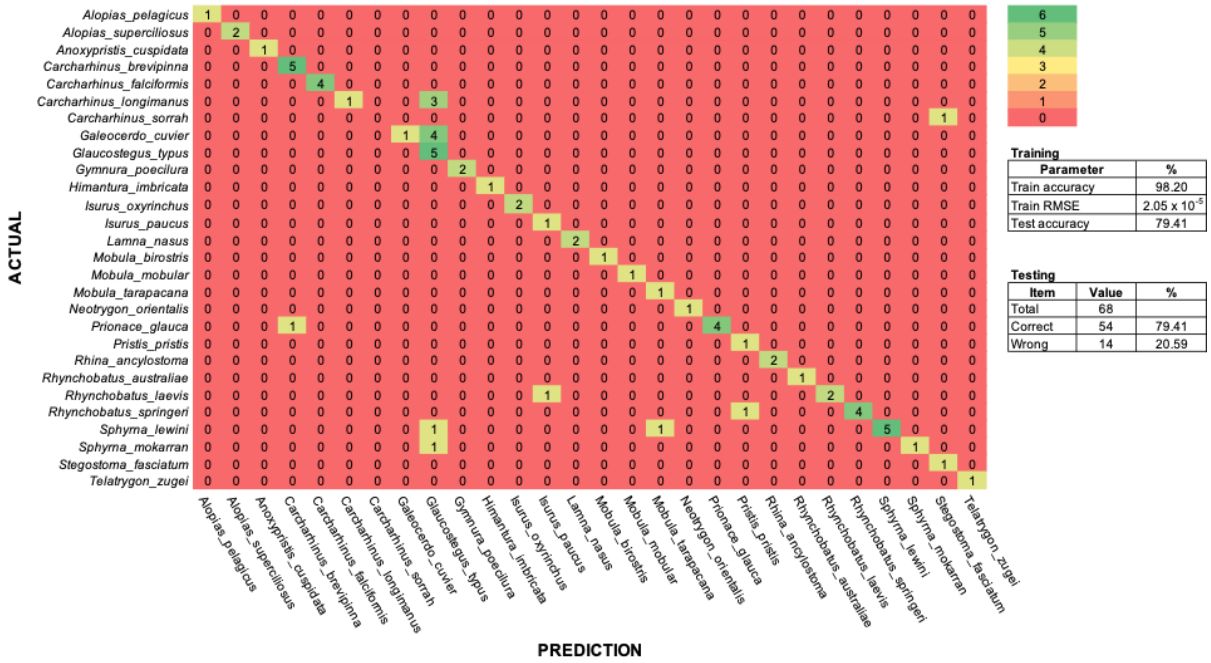

843

844 **Figure 5**. Confusion matrix of 28 shark and ray species assignment.

845

Tables

Table 1. Amplification conditions of each species using the targeted segments using the FASTFISH-ID technology. Amplification condition denotes whether the species amplified at either or both segments (BS1 and BS2) and whether the species was distinguishable from all other species by its fluorescent signature(s) and deep learning.

No.	CITES status	Scientific name	English name	Amplification Condition		Distinguishable	
				Barcode segment 1 (BS1)	Barcode segment 2 (BS2)	Visual	Deep Learning
1	Yes	*Alopias pelagicus*	Pelagic thresher	Yes	Yes	Yes	Yes
2		*Alopias superciliosus*	Bigeye thresher	Yes	Yes	Yes	Yes
3		*Carcharhinus falciformis*	Silky shark	Yes	No	No	Yes
4		*Carcharhinus longimanus*	Oceanic whitetip shark	No	Yes	Yes	No
5		*Isurus oxyrinchus*	Shortfin mako shark	No	Yes	Yes	Yes*
6		*Isurus paucus*	Longfin mako shark	Yes	Yes	Yes	Yes*
7		*Lamna nasus*	Porbeagle shark	No	Yes	Yes	Yes
8		*Sphyrna lewini*	Scalloped hammerhead	Yes	Yes	Yes	Yes
9		*Sphyrna mokarran*	Great hammerhead	Yes	Yes	Yes	Yes
10		*Carcharhinus brevipinna*	Spinner shark	Yes	No	Yes	Yes
11		*Carcharhinus sorrah*	Spot-tail shark	Yes	Yes	Yes	No
12		*Prionace glauca*	Blue shark	Yes	No	No	Yes*
13		*Anoxypristis cuspidata*	Knifetooth sawfish	Yes	Yes	Yes	Yes
14		*Glaucostegus typus*	Giant shovelnose ray	No	No	No	No
15		*Mobula birostris*	Giant oceanic manta ray	Yes	Yes	No	Yes
16		*Mobula mobular*	Giant devil ray	Yes	Yes	No	Yes
17		*Mobula tarapacana*	Sicklefin devil ray	Yes	Yes	Yes	Yes
18		*Pristis pristis*	Largetooth sawfish	No	Yes	Yes	Yes
19		*Rhina ancylostoma*	Bowmouth guitarfish	Yes	Yes	Yes	Yes

No.	CITES status	Scientific name	English name	Amplification Condition		Distinguishable	
				Barcode segment 1 (BS1)	Barcode segment 2 (BS2)	Visual	Deep Learning
20		*Rhynchobatus australiae*	Whitespotted guitarfish	Yes	Yes	Yes	Yes
21		*Rhynchobatus laevis*	Smoothnose wedgefish	No	Yes	Yes	Yes*
22		*Rhynchobatus springeri*	Broadnose wedgefish	Yes	Yes	Yes	Yes*
23	No	*Galeocerdo cuvier*	Tiger shark	No	No	No	No
24		*Stegostoma fasciatum*	Zebra shark	Yes	Yes	Yes	No
25		*Gymnura poecilura*	Longtail butterfly ray	Yes	Yes	Yes	Yes
26		*Himantura imbricata*	Bengal whipray	Yes	Yes	Yes	Yes
27		*Neotrygon orientalis*	Oriental bluespotted maskray	Yes	Yes	Yes	Yes
28		*Telatrygon zugei*	Pale-edged stingray	Yes	Yes	Yes	Yes
Total distinguishable species						**22**	**23**

Note: species with Asterix "" mark have probability of mis-assignment by the deep learning model*

852